

XPS Investigation of TiO₂/ZrO₂/SiO₂ Films Modified with Ag/Au Nanoparticles

Mindaugas ANDRULVIČIUS^{1*}, Sigita TAMULEVIČIUS^{1,2}, Yuriy GNATYUK³,
Nadija VITYUK³, Natalia SMIRNOVA³, Anna EREMENKO³

¹Institute of Physical Electronics of Kaunas University of Technology, Savanoriu 271, Kaunas LT-51368, Lithuania

²Department of Physics, Kaunas University of Technology, Studentų 50, LT-51368 Kaunas, Lithuania

³O. Chuiko Institute of Surface Chemistry of NASU, 17 Gen. Naumov str., 03164, Kyiv, Ukraine

Received 28 September 2007; accepted 07 November 2007

Nanocomposites of inorganic nanoparticles have attracted considerable attention recently. In present work TiO₂/ZrO₂/SiO₂ ternary films have been prepared using low-temperature sol-gel method. Corresponding alkoxides were used as titanium, zirconium and silicon sources and acetylaceton as complexing agent. The films were deposited onto titanium substrates using dip-coating technique. Samples modified with metal nanoparticles were prepared by adding appropriate metal source into the sol. Subsequent thermal treatment of the films led to crystallization of oxide matrix with incorporated metal nanoparticles, which was monitored by the appearance of the surface plasmon band of Au/Ag metal particles in the UV-VIS spectra of the films. Chemical composition of the films was investigated by X-ray photoelectron spectroscopy (XPS). Films of single, double, triple oxides and triple oxides modified with noble metals were investigated. Comparison of peaks positions in single, double and triple systems led to assumption that produced TiO₂/ZrO₂/SiO₂ films are ternary oxides. It was found that the negative shift of the O 1s peak of oxygen bounded to silicon depends mostly on Ti content in the mixed oxides films. Correlation between oxygen O 1s peak shift, optical band gap decrease and catalytical activity of the films was noticed.

Keywords: XPS, TiO₂/ZrO₂/SiO₂ films, noble metal nanoparticles.

INTRODUCTION

Titanium dioxide photocatalysis presents advanced technology to clean environment on pollutant traces different in origin (organics, inorganic ions) as well as from biological objects as bacteria, viruses, etc. Recently, self-cleaning and superhydrophobic coatings based on TiO₂ attracted a lot of attention from science and industry. It is known that TiO₂ effectiveness could be improved by mixing with other oxides (ZrO₂, SiO₂) that control structure-sorption, optical and electronic properties. Variety of applications has been proposed for mixed oxides based on TiO₂: catalysis [1] and photocatalysis [2], chemical resistance coatings, anti-reflective films, etc.

Metal nanoparticles themselves have unique characteristics because of their large surface area-to-volume ratio and therefore nanocomposites of inorganic nanoparticles have attracted considerable attention [3, 4]. Metal nanoparticles embedded in dielectric matrices are promising composite materials for optical applications as systems with enhanced third-order electronic susceptibility $\chi^{(3)}$ [5]. Semiconductor-metal composite nanoparticles have been shown to facilitate charge separation in the semiconductor nanostructures that is beneficial for maximizing the efficiency of photocatalysis reactions [6].

Sol-gel technology is one of the most practically accepted techniques to prepare complex oxide mixtures with atomic level mixing of the components. In this work we present the XPS analysis of ternary TiO₂/ZrO₂/SiO₂ films prepared by sol-gel method and modified with noble metal nanoparticles. Single and binary oxides were also investigated to elucidate observed shifts of binding energy

values and thus to control formation of chemical bonds between components.

EXPERIMENTAL

TiO₂/ZrO₂/SiO₂ ternary films have been prepared using low-temperature sol-gel method [7]. Corresponding alkoxides were used as titanium, zirconium and silicon sources and acetylaceton as complexing agent. Composition of the samples that were prepared and investigated in this study is presented in the second line of the Table 1. Dip-coating technique was applied for film deposition onto titanium substrates for XPS measurements and onto quartz/glass substrates for optical/structural investigations. The films were treated up to 500 °C in air to burn out organic residuals from the gel and to form an oxide network.

The samples modified with metal nanoparticles were prepared by adding appropriate metal source (AgNO₃, HAuCl₄) into sol for film deposition. Subsequent thermal treatment of the films led to crystallization of the oxide matrix with incorporated metal nanoparticles when carbon containing residuals acted as reducing agent. Formation of the Au/Ag metal nanoparticles was monitored by the appearance of surface plasmon band in the UV-VIS spectra.

Chemical composition of the films was investigated by X-ray photoelectron spectroscopy method (XPS) employing KRATOS ANALYTICAL XSAM-800 spectrometer. TiO₂, ZrO₂ and SiO₂ oxide films, mixed oxides films and mixed oxides films with noble metals were investigated. Surface atomic concentrations of the films were calculated using KRATOS DS800 software from appropriate peak area. Surface charging effects for all detailed spectra were corrected assuming that the carbon atmospheric contami-

*Corresponding author. Tel.: +370-37-313432; fax.: +370-37-314423.
E-mail address: mindaugas.andrulevicius@fei.lt (M. Andrulevičius)

nant peak is at 284.75 eV position. Fitting procedures for the XPS spectra were performed employing XPSPEAK 4.1 software.

UV-VIS absorption spectra of the films deposited onto quartz substrates were recorded by Perkin-Elmer Lambda Bio-40 spectrophotometer in the 190 nm – 1000 nm wavelength range. Wide-angle XRD spectra of the films deposited onto glass slides and heat treated up to 600 °C were investigated by DRON-4-07 spectrometer with CuK_α irradiation.

RESULTS AND DISCUSSIONS

Optical properties. Calcination of the films up to 500 °C in air environment leads to the completion of hydrolysis and condensation reactions with formation of the oxide network. Prepared samples are transparent, homogeneous and abrasion resistant with thickness ~ 100 nm. Absorption spectra of the single and binary films on quartz substrates are presented in Fig. 1.

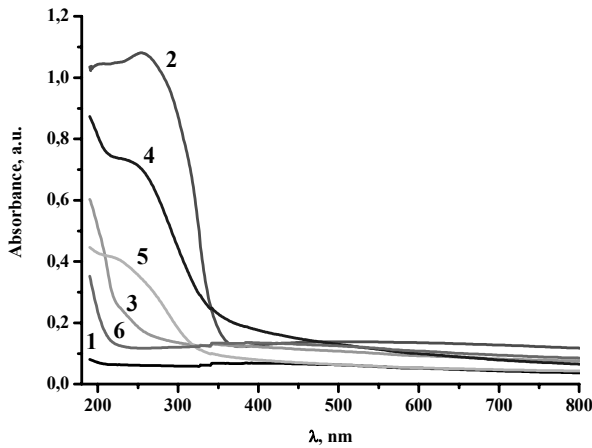


Fig. 1. Optical absorption spectra of the films after heat treatment at 500 °C: 1 – SiO_2 , 2 – TiO_2 , 3 – ZrO_2 , 4 – $\text{TiO}_2/\text{ZrO}_2$, 5 – $\text{SiO}_2/\text{TiO}_2$, 6 – $\text{SiO}_2/\text{ZrO}_2$

Optical spectra of the pure oxide films (Fig. 1, curves 1 – 3) demonstrate absorption edge shift into red wavelength region going over from SiO_2 to TiO_2 that corresponds to changes of the band gap energies E_g of Si, Zr and Ti oxides [8, 9]. SiO_2 mixing with TiO_2 or ZrO_2 (Fig. 1, curves 5, 6) causes appearance of the absorption in the near UV spectral range due to the electronic transitions corresponding to the ligand-to-metal charge transfer under electron excitation from valence band to conduction band. This phenomenon witness's silica films sensitization to lower energy light, which is especially the case for $\text{SiO}_2/\text{TiO}_2$ films. On the other hand, when titanium dioxide is doped with ZrO_2 (Fig. 1, curve 4) blue shift of the absorption edge could be observed that corresponds to the increase of the E_g value for the TiO_2 due to the quantum size effect development for smaller crystallites. It is known that titanium dioxide crystallization and crystallites growth are inhibited in the presence of SiO_2 , ZrO_2 or Al_2O_3 [10]. The same features are characteristic for the $\text{SiO}_2/\text{ZrO}_2$ and $\text{SiO}_2/\text{TiO}_2$ films' spectra when comparing with the spectra of pure TiO_2 and ZrO_2 films.

In the Fig. 2 optical absorption spectra of ternary systems with different content of the components are

presented. It is clearly seen that varying ratio of the components, namely titanium dioxide content increase, one can change optical properties of ternary $\text{TiO}_2/\text{ZrO}_2/\text{SiO}_2$ films. Red shift of the absorption band edge for the system with higher TiO_2 content (Fig. 2, curve 2) reveals TiO_2 crystallites growth. Band gap energy values calculated according to the position of the absorption band edge are presented in the Table 1 below.

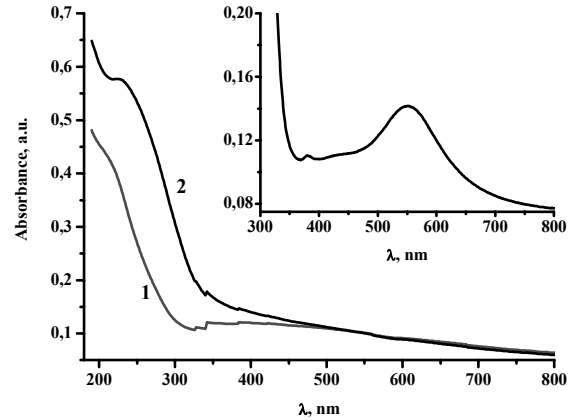


Fig. 2. Optical absorption spectra of the films after heat treatment at 500 °C: 1 – $\text{TiO}_2/\text{ZrO}_2/\text{SiO}_2$ (70 % SiO_2), 2 – $\text{TiO}_2/\text{ZrO}_2/\text{SiO}_2$ (30 % SiO_2). Inset: $\text{TiO}_2/\text{ZrO}_2/\text{SiO}_2$ (70 % SiO_2)/3.4 % Au film optical absorption spectrum

One-step method of preparation of TiO_2 films with embedded noble metal nanoparticles has been developed in our laboratory earlier [11]. Here we introduce silver and gold nanoparticles into ternary $\text{TiO}_2/\text{ZrO}_2/\text{SiO}_2$ films to obtain system with increased photocatalytic activity and interesting for optics.

Heat treatment of the films up to 500 °C with introduced metal sources led to simultaneous formation of the oxide network and metal nanoparticles. This can be easily monitored by the appearance of the surface plasmon bands for Ag and Au nanoparticles in the absorption spectra (Fig. 2, inset).

XRD analysis. XRD analysis of ternary systems did not give clear information about crystalline structure of the composites. This is more likely due to the insufficient resolution of XRD method used for investigation of the nanosized systems than due to the formation of amorphous oxide network. In the XRD spectra of pure TiO_2 and ZrO_2 films (Fig. 3) deposited onto glass substrates and heat treated at 600 °C can be distinguished reflections corresponding to the TiO_2 anatase and tetragonal ZrO_2 phases. As it was discussed previously common crystallization in the binary or ternary systems during oxide network formation causes inhibitive influence on the growth and agglomeration of the individual phases of the components, partly even due to the chemical interaction between components with formation of Ti-O-Si, Ti-O-Zr and Si-O-Zr bonds. Vogel et al [12] also reported formation of tiny crystallites of TiO_2 after calcination even at 350 °C. These titanium dioxide crystallites embedded into amorphous oxide network were “amorphous for XRD” and detected by electron diffraction and bright field TEM.

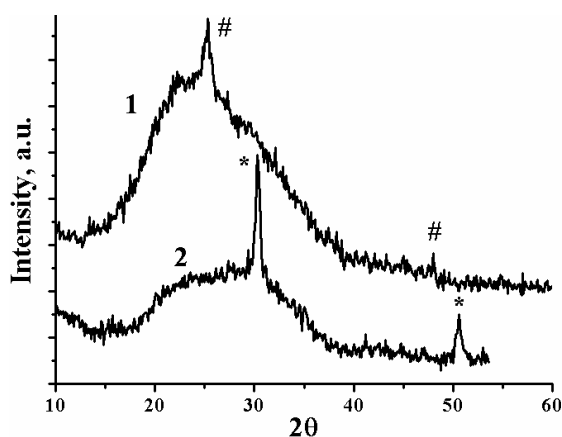


Fig. 3. XRD spectra of TiO₂ (1) and ZrO₂ (2) films deposited onto glass substrates and heat-treated at 600 °C: # – TiO₂ anatase phase related peaks, * – tetragonal ZrO₂ related peaks

Photoactive phase formation in our systems (that is due to TiO₂ nanocrystallites formation) was also proved indirectly by analysis of photocatalytic activity of ternary TiO₂/ZrO₂/SiO₂ films in the process of Cr(VI) ions photo reduction to Cr(III) state (it will be published in following article).

XPS investigation. Formation of chemical bonds between components in binary and ternary oxide mixtures was investigated using XPS method. For this purpose detailed spectra of binary and ternary sol-gel films and pure oxides were investigated and compared. The surface of the ternary oxide films modified with noble metals nanoparticles were investigated also. In addition the comparison of wide spectra of samples were made to insure that all peaks are properly detected by XPS method.

Calculated surface atomic concentrations of the synthesized films and molar concentration of used ingredients are presented in the Table 1. In the first column the peak, which was used for concentration calculations, is indicated (locations of these peaks can be found in wide spectra in Fig. 4 and Fig. 5). The carbon surface atomic

concentration, which varied from 13 % to 18 % for ternary oxide mixtures, is not included in this table. Oxygen concentration for the single oxides only is given for data clearance. Deviations from the calculated surface composition and initial molar concentrations apparent in this table can be related to the differences in hydrolysis rates of the precursor components. As the result difference in the constituents' distribution over film profile can be predicted.

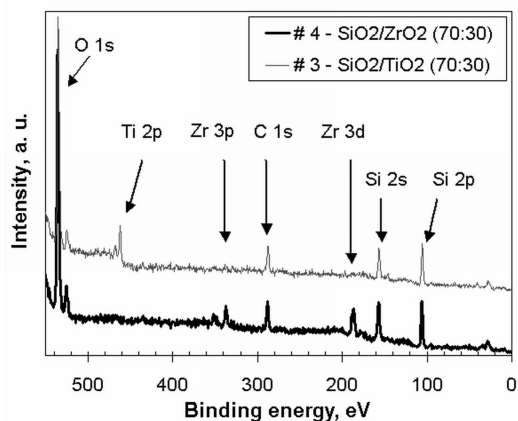


Fig. 4. Wide XPS spectra of silicon – zirconium and silicon – titanium binary oxides (all wide spectra are presented without charge effects compensation)

From the Table 1 one can see that the oxygen surface atomic concentration in single oxides exceeds the theoretical values (66.6 %) by 6.1 %, 5.4 %, 6.2 % and 5.2 % for TiO₂, ZrO₂, SiO₂ films and quartz sample respectively (quartz sample were analyzed but not shown in Table 1). This disagreement can arise due to presence of small amount of oxygen based atmospheric contaminants on the surface of investigated films and quartz since samples were not sputtered before the XPS analysis.

Atmospheric contaminants are indirectly confirmed by presence of typical carbon contaminant peak C 1s at 284.7 eV in binding energy scale that was observed for all samples (see Fig. 4 and Fig. 5) and in the quartz sample

Table 1. Calculated surface atomic concentrations of synthesized films and initial molar concentrations.

Sample Number	# 1	# 2	# 3	# 4	# 5	# 6	# 7	# 9	# 10	# 11
Elements and molar conc., %	TiO ₂	TiO ₂ /ZrO ₂ (70:30)	SiO ₂ /TiO ₂ (70:30)	SiO ₂ /ZrO ₂ (70:30)	TiO ₂ /ZrO ₂ /SiO ₂ (21:9:70)	TiO ₂ /ZrO ₂ /SiO ₂ (49:21:30)	TiO ₂ /ZrO ₂ /SiO ₂ (21:9:70) 5 % Ag	TiO ₂ /ZrO ₂ /SiO ₂ (21:9:70) 3.4 % Au	ZrO ₂	SiO ₂
Peak	Surface atomic concentration									
O 1s	72.7 %								72.0 %	72.8 %
Ti 2p	27.3 %	73.7 %	20.4 %		26.3 %	36.4 %	17.7 %	20.8 %		
Zr 3d		26.3 %		9.9 %	6.1 %	9.9 %	5.2 %	4.7 %	28.0 %	
Si 2p			79.6 %	90.1 %	67.6 %	53.7 %	62.8 %	74.0 %		27.2 %
Au 4f								0.4 %		
Ag 3d							14.3 %			
	<i>E_g</i> , eV									
	3.49	3.61	3.75	5.72	4.04	3.68	3.80	3.87	5.43	>6.2 (8.9*)

* literature data in [9].

as well. In addition, the presence of carbon containing residuals in the films treated at 500 °C can not be denied taking into account DTA/TG analysis of the corresponding powders (not shown here). It was observed continuous weight loss of the samples under heating up to 600 °C that was related to the burnout of the organic residuals of the gel.

Wide XPS spectra of the investigated films are presented in Fig. 4 and Fig. 5. The constant number of counts per second was added to all lines of spectra to overcome overlapping data points.

Two main peaks for silicon (Si 2s and Si 2p) and two peaks for zirconium (Zr 3p and Zr 3d) were detected in the binary SiO₂ oxides spectra (Fig. 4). For titanium only one main peak (Ti 2p doublet) at 461 eV (Fig. 4) and small Ti 3p peak at 38 eV was detected (Fig. 5, a, sample # 2).

Appearance of appropriate peaks of main elements for single, binary, ternary oxides and ternary oxides modified with noble metals can be seen in wide spectra in Fig. 5, a and b. Zirconium Zr 3p and Zr 3d peaks appearance in ternary oxides (Fig. 5) is especially important since the XRD analysis of ternary systems did not give clear information about the ZrO₂ crystalline phase as mentioned above.

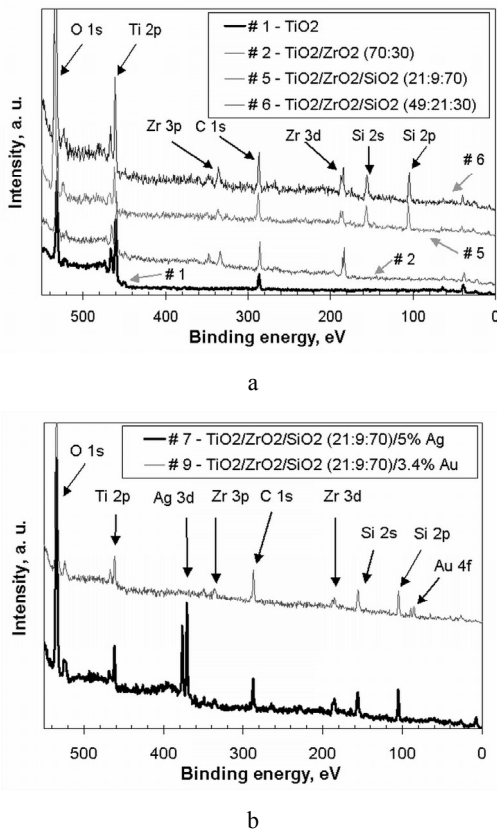


Fig. 5. Wide XPS spectra: a – single oxide TiO₂ and mixed binary or ternary oxides; b – ternary oxides modified with noble metal nanoparticles (all wide spectra are presented without charge effects compensation)

The detailed XPS spectra of oxygen for single, binary and ternary oxide films are compared in Fig. 6. In oxygen O 1s and silicon Si 2p regions (Fig. 6, inset) one can see that the positions of O 1s and Si 2p peaks for Si-O bonds are negative shifted and this shift depends on titanium and

zirconium content in the mixed oxides. The results of calculated peaks shifts (relative to single SiO₂ in sample # 11) are summarized in Table 2 and illustrated in Fig. 7. In sample # 11 oxygen O 1s and silicon Si 2p peaks position (532.9 eV and 103.44 eV respectively) coincides with known [13] peak positions in SiO₂: O 1s peak – 532.89 eV and Si 2p peak – 103.6 eV.

Table 2. O 1s and Si 2p peaks shift dependence on titanium and zirconium atomic concentration

Num.	Composition and molar conc., %	Atomic conc., %		Peak shift, eV	
		Zr	Ti	Si 2p peak (SiO ₂)	O 1s peak (SiO ₂)
# 11	SiO ₂ (100)	0	0	0	0
# 4	SiO ₂ /ZrO ₂ (70:30)	9.9	0	-0.31	-0.260
# 7	TiO ₂ /ZrO ₂ /SiO ₂ (21:9:70) 5% Ag	5.2	17.7	-0.76	-0.494
# 3	SiO ₂ /TiO ₂ (70:30)	0	20.4	-0.51	-0.355
# 9	TiO ₂ /ZrO ₂ /SiO ₂ (21:9:70) 3.4% Au	4.7	20.8	-0.68	-0.490
# 5	TiO ₂ /ZrO ₂ /SiO ₂ (21:9:70)	6.1	26.3	-0.71	-0.485
# 6	TiO ₂ /ZrO ₂ /SiO ₂ (49:21:30)	9.9	36.4	-1.03	-0.720

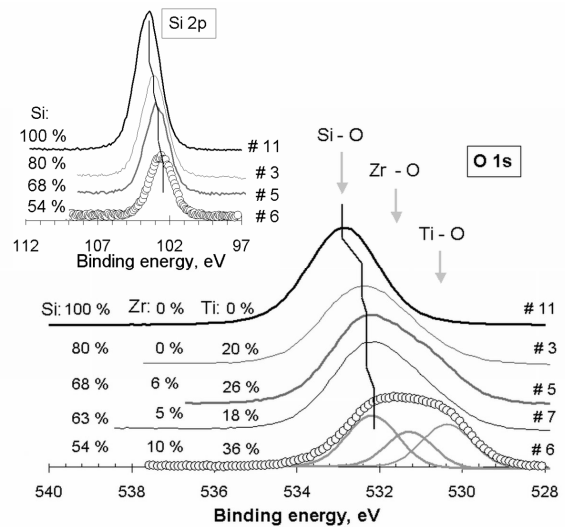


Fig. 6. Detailed XPS O 1s region spectra for sol-gel prepared pure and mixed SiO₂ films (Si 2p region spectra is shown in the inset on the left). At the bottom of picture O 1s spectra of sample # 6 is fitted into three peaks corresponding to the appropriate oxygen bonds as indicated by gray arrows at the top

From the Fig. 6 and Table 2 it can be seen that the shift of Si 2p peak is 0.51 eV in sample # 3 and 1.03 eV in sample # 6 then Ti atomic concentration changes from 0 % to 20 % and 36 % respectively. Such peak position shift suggests its uniform dependence on the Ti concentration (see Fig. 7, b).

On the other hand atomic concentration of Ti in sample # 3 (20 %) slightly decreases to 18 % in sample # 7 but O 1s and Si 2p peak positions changes in opposite direction. This can indicate influence of appearance of Zr and/or Ag nanoparticles. Meanwhile 48 % increase of Ti concentration and 17 % increase of Zr concentration (samples # 7 and # 5) resulted in smaller shift of Si and O peaks. Therefore influence on peak position in sample # 7 can be attributed mainly to the presence of Ag nanoparticles.

Described above peaks shifts are in good agreement with red shift of optical absorption for single and mixed oxides (see Fig. 1 and Fig. 2) and E_g reduction from 8.9 eV to 3.68 eV (see Table 1, bottom row). The optical absorption red shift dependence on TiO_2 concentration for ternary oxides also was mentioned above (see Fig. 2). It can be mentioned also that Si 2p and O 1s peaks position shift dependence correlates well with the photocatalytic activity of investigated films.

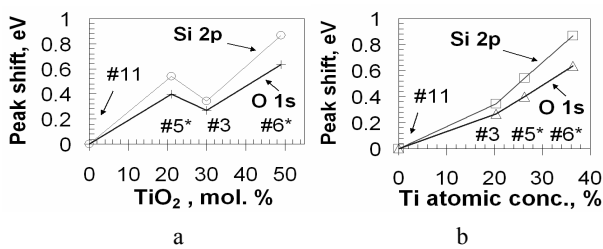


Fig. 7. Shift of silicon and oxygen peaks for Si-O bounds in single, binary and ternary oxides films: a – dependence on titanium initial molar concentration, b – dependence on titanium surface atomic concentration. Circles and squares – the Si 2p peak shift; crosses and triangles – the O 1s peak shift. On the bottom the sample numbers (see Table 1.) are presented where asterisk indicates ternary oxide. Negative peaks shift values were converted to positive ones for picture clearance. Lines are drawn for eyes guidance only

Comparing Fig. 7, a and b, one can see that data presented in 7, b, are in more uniform dependence (peak shift of surface atomic concentration) versus molar concentration. In both figures obvious similarity between silicon and oxygen peaks position evolution can be noticed.

Titanium XPS Ti 2p region spectra is presented in Fig. 8, a. In the spectrum of the sample # 1 two main peaks of Ti 2p doublet are shown where position of more intense peak Ti $2p_{3/2}$ at 458.65 eV is in good agreement with known value (458.68 eV) for pure TiO_2 [13]. In this figure the main Ti $2p_{3/2}$ peak position dependence (positive shift relative to position of Ti $2p_{3/2}$ peak in single TiO_2 , sample # 1) on titanium content in the films can be noticed. Ti $2p_{3/2}$ peak is shifted by 0.66 eV for the sample # 7 and by 0.87 eV for sample # 3 (see Fig. 8, b). Similar shifts were found for other samples (not shown in Fig. 8, a) as well: 0.31 eV for the sample # 6, 0.64 eV – for # 9 and 0.68 eV for # 5. This demonstrates almost uniform peak position dependence on Si/Ti relative atomic concentration (Fig. 8, b). The opposite effect was noticed for the sample # 2 where Ti $2p_{3/2}$ peak shifted by -0.1 eV (negative shift) was found. The latest observation can be attributed to the formation of binary $\text{TiO}_2/\text{ZrO}_2$ oxide.

Positive shift for Ti $2p_{3/2}$ peak is described in [14] where electron beam evaporated single TiO_2 and binary

oxides ($\text{TiO}_2/\text{SiO}_2$) are investigated (Fig. 8, b, thick line with circles). In the article positive shifts (relative to single oxide TiO_2) of 0.17 eV, 0.27 eV and 0.87 eV are reported for the mixed oxides with 82 %, 56 % and 24 % of Ti contents respectively [14]. From the reported results it's clear that the main Ti $2p_{3/2}$ peak positive shift depends on the titanium content in the binary oxide. Similar peak shift dependence on Ti content was observed in our experiments for $\text{TiO}_2/\text{SiO}_2$ oxides films (Fig. 8, a and b) indicating Ti-O-Si or Ti-O-Zr bonds formation. Therefore shift dependence in our experiment can be attributed to binary oxides formation. Addition of noble metals showed only negligible effect on the Ti $2p_{3/2}$ peak position.

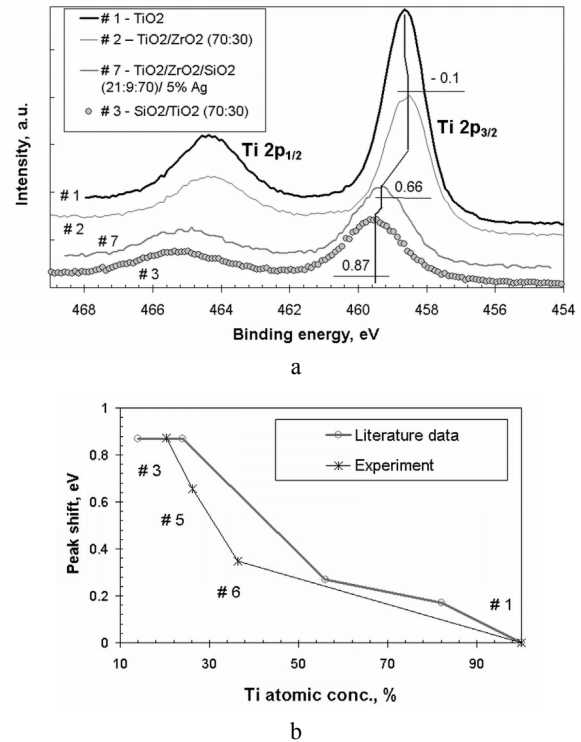


Fig. 8. Detailed titanium XPS Ti 2p region spectra for sol-gel prepared single and mixed oxide films and the peak shift dependence: a – Ti 2p region spectra for sol-gel prepared single and mixed oxide films; b – titanium Ti $2p_{3/2}$ positive peak shift dependence on titanium surface concentration in single and mixed oxide films: thick line with circles – $\text{TiO}_2/\text{SiO}_2$ literature data [14]; thin line with asterisks – calculated experimental data of positive peak shift relative to peak position in sample # 1 (sample numbers correspond to Table 1, lines are drawn for eyes guidance only

In the Fig. 9 the zirconium detailed XPS spectra is shown. In this figure Zr $3d_{5/2}$ peak position for mixed oxides is shifted towards higher binding energies (positive shift) when compared to peak position in sample # 10 for sol-gel prepared ZrO_2 film. In the sample # 2 the Ti 2p peak (Fig. 8) and Zr 3d peak (Fig. 9) positions shift in opposite directions. Similar shifts behavior can be noticed for Si 2p – Ti 2p and Si 2p – Zr 3d peaks therefore these shifts can be attributed to the formation of binary and ternary oxides as was discussed above.

Also it should be noticed that sol-gel prepared ZrO_2 film (sample # 10) showed significant negative Zr $3d_{5/2}$ peak shift by -0.71 eV when compared to known values in

[13]. The negative Zr 3d_{5/2} peak shift dependence on ZrO₂ phase and nanocrystallites size is described in [15] where pure ZrO₂ powder was prepared by thermal hydrolysis and additional thermal treatment. Nanocrystallites size there varied from 107 nm to 6 nm in five steps while the Zr 3d peak position was negative shifted from 0.6 eV to 1.42 eV respectively comparing to Zr 3d_{5/2} peak position in bulk ZrO₂. Therefore negative shift in the sample # 10 can be attributed to the formation of nanocrystallites in the sol-gel prepared film. Comparing data in [15] and Zr 3d_{5/2} peak position shift by 0.71 eV in sol-gel film the formation of nanocrystallites with sizes in the range of 25 nm – 90 nm in sample # 10 can be estimated. Another similarity of the sample # 10 to the experiment described in literature is nanocrystalline phase formation. In the article [15] ZrO₂ phase transition from cubic to tetragonal occurs near 3 nm and that from tetragonal to monoclinic corresponds to nanocrystallites critical size of 25 nm. In the sample # 10 only tetragonal phase was detected (Fig. 3, 2) by XRD method. Therefore described above very rough approximation of the nanocrystallite size (from 25 nm to 90 nm) now can be revised and it could estimate from 20 nm to 30 nm when both XPS and XRD results are compared.

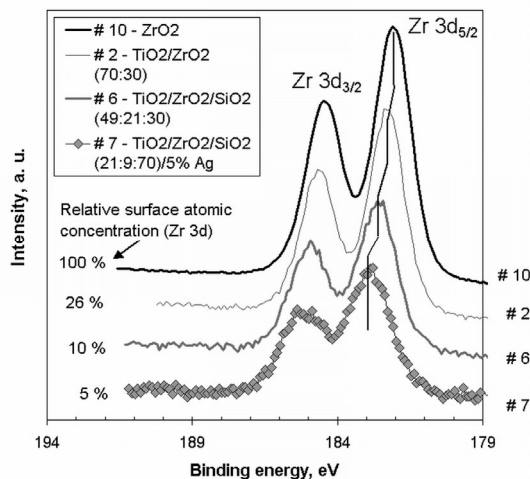


Fig. 9. Detailed zirconium XPS spectra for sol-gel prepared pure and mixed oxides films. On the left side calculated relative zirconium surface atomic concentration is given (see Table 1)

The XPS spectra of silver and gold nanoparticles in ternary oxide films are presented in Fig. 10 and Fig. 11 respectively. In silver Ag 3d region the fitted spectra consist of two main peaks – Ag 3d_{5/2} and Ag 3d_{3/2} doublet. Ag 3d_{5/2} peak position at 367.99 eV (Fig. 10, thick line) is in good agreement with 368.196 eV reported in [13], 368.22 eV in [16] and 367.98 eV in [17] for metallic silver. In this figure fitted peaks of smaller intensity are located on the right side of main peaks. Separation of these peaks from metallic peak position is approximately 0.3 eV and is coincident with known separation values for silver oxide Ag₂O [13, 17], therefore they can be attributed to Ag₂O. Low intensity satellite at 364.5 eV is typical for nonmonochromatized Al K α excitation source [17].

Fitting procedure results for gold Au 4f region is presented in Fig. 10. In this figure the literature data

reported in [17] are compared with the experimental data. Peaks corresponding to gold oxide were not detected. Small shift of Au 4f_{7/2} peak by 0.2 eV towards lower binding energy values was found.

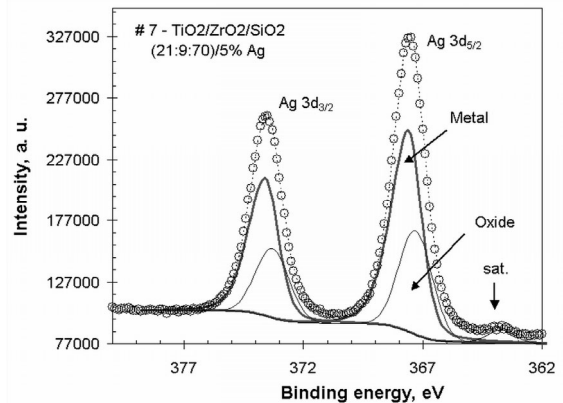


Fig. 10. Fitting procedure for Ag 3d spectra for sample # 7 of mixed oxides film modified with silver nanoparticles TiO₂/ZrO₂/SiO₂ (21:9:70)/5 % Ag: circles – experimental data, dashed line – fitted curve; thick line – metallic silver, thin line – silver oxide

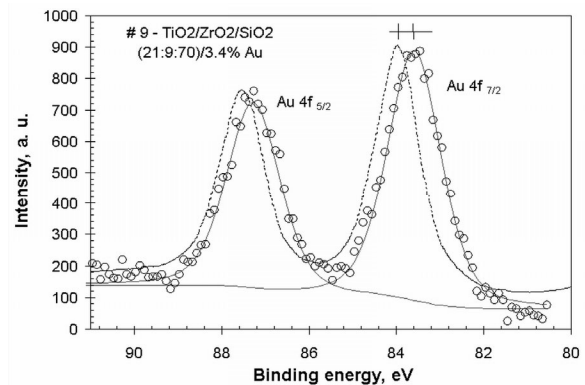


Fig. 11. Fitted Au 4f spectra of sample # 9 TiO₂/ZrO₂/SiO₂ (21:9:70)/3.4 % Au and gold reference spectra: circles – experimental data, thin lines – fitted curve; dashed line – literature data [17]

Gold Au 4f doublet peaks were detected by XPS at sufficient intensity, peaks position and shape (Fig. 10) coincide with literature data [17] nevertheless considerable disagreement between Au molar and surface atomic concentrations was found (Table 1). This disagreement can be related to the differences in Au concentration over the film profile.

CONCLUSIONS

Optical analysis by UV-VIS showed E_g dependence on the film content comparing single, binary and ternary oxide films. Formation of noble metal nanoparticles in ternary oxide films was also confirmed by UV-VIS analysis.

Formation of TiO₂ anatase and tetragonal ZrO₂ phases in the single oxides was found by XRD analysis. However no crystalline phase corresponding to ZrO₂ was detected in the ternary oxides by XRD.

In wide XPS spectra of investigated samples the main peaks of appropriate elements were detected. Some marginal disagreement was found between the molar

concentration and calculated surface atomic concentrations for main elements except gold. In the XPS wide spectra the Zr 3d and Zr 3p peaks were found despite no crystalline phase corresponding to ZrO₂ was detected in XRD analysis of ternary oxides. In detailed XPS spectra O 1s, Si 2p and Ti 2p peaks positions showed good agreement with literature data for analyzed single SiO₂ and TiO₂ oxides.

From the detailed XPS spectra it was found that the O 1s and Si 2p peaks positions in Si-O bounds depend on titanium and zirconium content in the mixed oxide films demonstrating approximately uniform dependence on Ti and Zr surface atomic concentration. On the other hand the 48 % increase of Ti and 17 % increase of Zr atomic concentrations resulted in smaller shift of Si and O peaks then addition of 5 % of Ag to the same film. This indicates strong sensitivity of Si and O peaks positions in ternary films to noble metal nanoparticles addition. Detected by XPS oxygen and silicon peak positions evolution correlates with E_g reduction of analyzed mixed oxides and with the photocatalytic behavior of the films as well.

Almost linear Ti 2p_{3/2} peak position dependence on Ti content in mixed TiO₂/SiO₂ oxides was noticed. Comparison with similar literature data disclosed Ti-O-Si bonds formation and lead to assumption of binary oxide formation.

In the fitted silver Ag 3d spectra, the Ag₂O chemical bonds were found out. Considerable disagreement between Au and Ag molar concentrations and surface atomic concentrations can be related to the differences in Au and Ag concentration over film profile and need to be further investigated.

Peak positions in XPS detailed spectra for analyzed mixed oxides showed strongly related character. Comparison to the literature data allowed us to assume that sol-gel prepared films are binary and ternary oxides.

E_g reduction (optical approach) and oxygen O 1s or Si 2p peaks negative shift (XPS approach) can be used as adequate indication for photocatalysis suitability of mixed silicon oxides.

Acknowledgments

This work was partly supported by the Lithuanian Science and Study Foundation.

REFERENCES

1. Xiao, F.-S., Han, Y., Yu, Y., Meng, X., Yang, M., Wu, S. Hydrothermally Stable Ordered Mesoporous Titanosilicates with Highly Active Catalytic Sites *J. Am. Chem. Soc.* 124 2002: pp. 888 – 889.
2. Fu, X., Clark, L. A., Yang, Q., Anderson, M. A. Enhanced Photocatalytic Performance of Titania-Based Binary Metal Oxides: TiO₂/SiO₂ and TiO₂/ZrO₂ *Environ. Sci. Technol.* 30 1996: pp. 647 – 653.
3. Mizukoshi, Y., Makise, Y., Shuto, T., Hu, J., Tominaga, A., Shironita, S., Tanabe, S. Immobilization of Noble Metal Nanoparticles on the Surface of TiO₂ by the Sonochemical Method *Ultrasonics Sonochemistry* 14 2007: pp. 387 – 392.

4. Miyazaki, Y., Shiratori, S. Preparation of Noble Metal Nanoparticles @ Titania Precursor Composite Electrostatic Self-assembled Film *Thin Solid Films* 499 2006: pp. 29 – 34.
5. Shiliang Q., Yawen Zhang, Huajun Li, Jianrong Qiu, Congshan Zhu. Nanosecond Nonlinear Absorption in Au and Ag Nanoparticles Precipitated Glasses Induced by a Femtosecond Laser *Optical Materials* 28 2006: pp. 259 – 265.
6. Subramanian, V., Wolf, E., Kamat, P. V. Semiconductor – Metal Composite Nanostructures. To What Extent Do Metal Nanoparticles Improve the Photocatalytic Activity of TiO₂ Films? *J. Phys. Chem. B.* 105 2001: pp. 11439 – 11446.
7. Eremenko, A., Smirnova, N., Rusina, O., Linnik, O., Eremenko, T. B., Spanhe, L., Rechthaler, K. Photophysical Properties of Organic Fluorescent Probes on Nanosized TiO₂/SiO₂ Systems Prepared by the Sol-gel Method *Journal of Molecular Structure* 553 2000: pp. 1 – 7.
8. Lucovsky, G., Hong, J. G., Fulton, C. C., Stoute, N. A., Zou, Y., Nemanich, R. J., Aspnes, D. E., Ade, H., Schlom, D. G. Conduction Band States of Transition Metal (TM) High-k Gate Dielectrics as Determined from X-ray Absorption Spectra *Microelectronics Reliability* 45 2005: pp. 827 – 830.
9. Kamiyama, S., Miura, T., Nara, Y. Comparison Between SiO₂ Films Deposited by Atomic Layer Deposition with SiH₂[N(CH₃)₂]₂ and SiH[N(CH₃)₂]₃ Precursors *Thin Solid Films* 515 2006: pp. 1517 – 1521.
10. Kim, J., Song, K. C., Focillias, S., Pratsinis, S. E. Dopants for Synthesis of Stable Bimodally Porous Titania *J. Europ. Ceram. Society* 21 2001: pp. 2863 – 2872.
11. Gnatyuk, Yu., Manuilov, E., Smirnova, N., Huang, W., Eremenko, A. Sol-Gel Produced Mesoporous TiO₂/Ag Coatings Effective in Rhodamine B Photooxidation *NATO Science Series II Mathematics, Physics and Chemistry "Functional Properties of Nanostructured Materials"* R. Kassing et al. (eds.) 223 2006: pp. 485 – 490.
12. Vogel, R., Meredith, P., Kartini, I., Harvey, M., Riches, J., Bishop, A., Heckenberg, N., Trau, M., Rubensztein-Dunlop, H. Mesoporous Dye-Doped Titanium Dioxide for Micro-Optoelectronic Applications *CHEMPHYSICHEM.* 4 2003: pp. 595 – 603.
13. Wagner, Ch. D., Naumkin, A. V., Kraut-Vass, A., Allison, J. W., Powell, C. J., Rumble Jr., J. R. *NIST Standard Reference Database* 20, Version 3.4.
14. Netterfield, R. P., Martin, P. J., Pacey, C. G., Sainty, W. G., McKenzie, D. R., Auchterlonie, G. Ion-Assisted Deposition of Mixed TiO₂-SiO₂ Films *Journal of Applied Physics* 66 1805 1989.
15. Tsunekawa, S., Asami, K., Ito, S., Yashima, M., Sugimoto, T. XPS Study of the Phase Transition in Pure Zirconium Oxide Nanocrystallites *Applied Surface Science* 252 2005: pp. 1651 – 1656.
16. ISO 15472:2001. Surface Chemical Analysis – X-ray Photoelectron Spectrometers – Calibration of Energy Scales.
17. Wagner, C. D., Riggs, W. M., Davis, L. E., Moulder, J. F., Muilenberg, G. E. Handbook of X-ray Photoelectron Spectroscopy, Perkin-Elmer Corporation, Physical Electronics Division, Eden Prairie, Minn. 55344. 1979.

Presented at the National Conference "Materials Engineering'2007" (Kaunas, Lithuania, November 16, 2007)